CHEMISTRY OF MATERIALS

Article

pubs.acs.org/cm

Fabrication of the Tricontinuous Mesoporous IBN-9 Structure with Surfactant CTAB

Yunfeng Zhao,[†] Lan Zhao,[‡] Guangchao Wang,[‡] and Yu Han*[,†]

[†]Advanced Membranes and Porous Materials Center and [‡]Core Lab of Imaging and Characterization, King Abdullah University of Science and Technology, Thuwal 23955-6900, Saudi Arabia

ABSTRACT: IBN-9 is the first tricontinuous mesoporous material, consisting of three identical interpenetrating channels that are separated by a single continuous silica wall. It was originally synthesized using a specially designed surfactant as template. The need of special surfactant in the synthesis inhibits extensive investigation of this novel structure and its applications. We demonstrate in this study that such a complicated tricontinuous mesostructure can also be fabricated from the most common and commercially available surfactant cetyltrimethylammonium bromide (CTAB) with the help of polar organic additives, e.g., *n*-butanol. The role of *n*-butanol is to finely tune the surface curvature of the organic/inorganic interface during the cooperative self-assembly process. Electron microscopic techniques are employed to identify different mesostructures from the mixture. This study reveals the possibility of discovering unprecedented mesostructures from conventional surfactant−water−silicates systems.

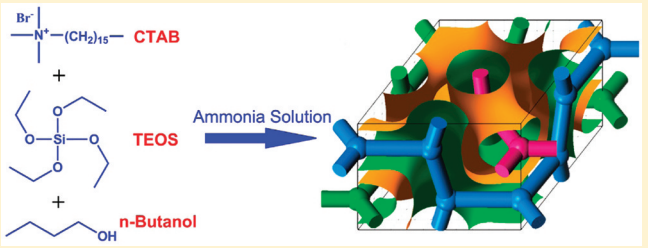

KEYWORDS: *mesoporous materials, tricontinuous structure, surfactant*

INTRODUCTION

The widespread applications of mesoporous materials in catalysis, separation, adsorption, and "hard-templating" synthesis rely on the precise control of their pore architectures,[1−9] compositions,[10−13] and surface properties.[14,15] Besides its fundamental significance, the fabrication of novel mesoporous structure also provides opportunities for developing new applications. During the last two decades, various mesoporous structures have been synthesized that can be roughly classified into three categories based on the pore types: cage, cylindrical channel, and bicontinuous channel. For mesoporous materials with cage-type pores, e.g., SBA-16[3] and FDU-12,[4] their structures can be considered as the packing of cages in different manners. For those with cylindrical channels, e.g., MCM-41[1] and SBA-15,[2] the one-dimensional (1D) channels are hexagonally arranged, forming a two-dimensional (2D) structure. Mesoporous materials with bicontinuous channels have more complicated structures, consisting of two identical three-dimensional (3D) channels that are interwoven with each other but separated by a single continuous pore wall. The pore wall can usually be described by a minimal surface.[5−7] For example, bicontinuous mesoporous material MCM-48 (cubic $Ia\bar{3}d$) has two interpenetrating chiral channels that are separated by a silica wall following the gyroidal (G) minimal surface;[5] likewise, AMS-10 (cubic $Pn\bar{3}m$) has two sets of four-connected channels and a continuous silica wall following the diamondoid (D) minimal surface.[6] Although the mesoporous structures are diverse, they can be correlated to each other by considering the surface curvature of their pore wall. Assuming that the pore diameters are comparable, the surface mean curvatures of different mesoporous structures follow the order: spherical cage > cylindrical channel > bicontinuous channel.[16] The surface curvature is significantly influenced by the molecular geometry of surfactant template as illustrated by $g = V/a_0 l$, where g is the surfactant packing parameter, V is the volume of the hydrophobic chain, a_0 is the effective area of the hydrophilic headgroup and l is the chain length.[17] In general, a smaller g value favors the formation of a mesostructure with higher surface mean curvatures. Specifically, ideal lamellar, bicontinuous, cylindrical, and spherical geometries have g values of 1, 2/3, 1/2, and 1/3, respectively.[17,18] Notably, besides the surfactant molecular geometry, other experimental conditions such as temperature, the types of counterions, the use of cosolvent, and especially the interaction from inorganic species, would also affect the packing of surfactant and thus the final mesostructure.

Recently, we synthesized a tricontinuous mesoporous material IBN-9 (hexagonal $P6_3/mcm$) and successfully resolved its structure by electron crystallography.[19−21] The results show that IBN-9 has a very complex structure, consisting of three identical 3D channels systems interwoven with each other but separated by a single continuous silica wall. This is very similar in concept to the well-known bicontinuous structures but more complicated because there is one more channel involved. IBN-9 is the first as well as the only tricontinuous mesoporous material reported up to now, and its structural analogies have

Received: August 12, 2011
Revised: November 1, 2011
Published: November 10, 2011

dx.doi.org/10.1021/cm2023983 | *Chem.Mater.* 2011, 23, 5250−5255

not been observed before even in soft matters such as surfactant-in-water and liquid crystal systems. The silica wall of IBN-9 follows perfectly a recently proposed branched hexagonal minimal surface, and it is the first representation of this minimal surface in real materials.[22] Moreover, IBN-9 shows unique nanofiber morphology with ultralong channels and ultrashort channels coexisting in one material.[19] Despite of these interesting features, IBN-9 has not been widely studied since it was reported, possibly because IBN-9 was synthesized by a specially designed surfactant (denoted as S2−C14, see Scheme 1) as template. The requirement of using a special noncommercially available surfactant much inhibits extensive investigation of this new structure and relevant studies. Therefore, it is highly desirable to develop new synthesis routes to enable the fabrication of this brand new mesostructure with simpler and commercially available surfactants. Herein, we report that the tricontinuous IBN-9 structure can be synthesized from the most common quaternary ammonium surfactant cetyltrimethylammonium bromide (CTAB).

Scheme 1. Surfactants Used for Synthesizing IBN-9: Specially Designed S2−C14 and Commercially Available CTAB

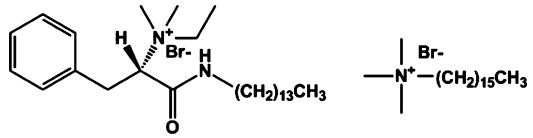

EXPERIMENTAL SECTION

In a typical synthesis of IBN-9 using CTAB as template, 50 mg CTAB was dissolved in 24 mL of aqueous ammonia solution (2.0 wt %, pH 11.35) at 45 °C, followed by the addition of 671 μL of *n*-butanol. Next, 250 μL of TEOS was added dropwise under a static condition. The final CTAB: n-Butanol: TEOS: NH_3: H_2O molar ratio in the synthesis mixture is 1: 53.5: 8.2: 205: 9706. The mixture was kept at 45 °C for 24 h under a static condition, and then aged at 100 °C in an autoclave for another 24 h. The obtained white precipitation was filtered, washed with water, and dried in air. To draw the synthesis space diagrams, the synthetic conditions including the ammonia concentration, the amount of butanol and the concentration of CTAB were systematically adjusted (see Figures 1a and 3a). The pH values of 1, 2, 5, 10, and 25 wt % ammonia solutions are 11.25, 11.35, 11.90, 12.32, and 13.17, respectively.

Transmission electron microscopy (TEM) and selected area electron diffraction (SAED) were performed on a FEI Titan electron microscope operated at 300 kV. Ultramicrotomy was conducted in a Leica EM UC6 system. Scanning electron microscope (SEM) was conducted on a FEI Quanta 600 electron microscope operated at 30 kV. Powder X-ray diffraction (XRD) patterns were collected on a Bruker D8 Advance diffractometer equipped with a NaI dynamic scintillation detector using Cu Kα radiation.

RESULTS AND DISCUSSION

In our previous work, we reported that three mesostructures, bicontinuous MCM-48, tricontinuous IBN-9, and 2-D hexagonal MCM-41, can be synthesized from ammonia solution by using surfactant S2−C14 as template and TEOS as silica source.[19,20] Both MCM-41 and MCM-48 were obtained under the exactly same conditions for IBN-9 synthesis except that lower surfactant concentration was used for the former while higher ammonia concentration was used for the latter.[19,20] For mesoporous silica synthesis in basic media, in general, higher pH and higher surfactant concentration are favorable conditions for the formation of mesostructure with lower surface mean curvature.[16] This is because under higher pH condition, the silicates will carry more negative charges which prompt a more compact packing of surfactant cations to keep the charge density matching.[23] Likewise, higher surfactant concentration also facilitates a more compact surfactant packing, leading to a lower surface curvature in the product.[16] According to the synthesis conditions, tricontinuous IBN-9 was inferred to have an intermediate surface mean curvature between the cylindrical MCM-41 and the bicontinuous MCM-48. This hypothesis was verified by calculating the surface mean curvatures of the three real mesostructures solved by electron crystallography.[19]

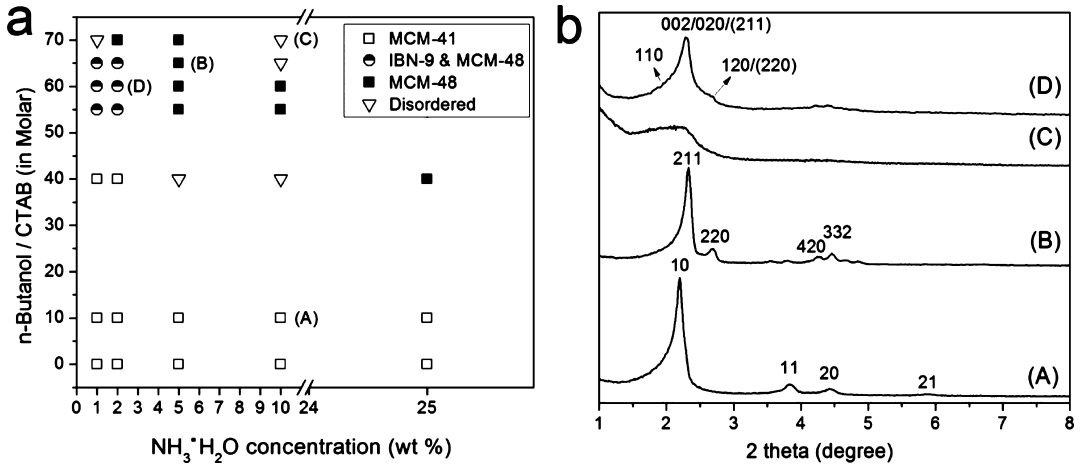

Figure 1. (a) Diagram of mesostructures synthesized from surfactant CTAB with varied amount of butanol and different ammonia concentrations, where each sample was synthesized using 0.25 mL of TEOS, 50 mg of CTAB in 24 mL aqueous ammonia solution at 45 °C. The representative conditions for the four types of products, i.e. MCM-41, MCM-48, disordered mesostructure and the mixture of IBN-9/MCM-48, are labeled with A−D, respectively, and (b) their corresponding indexed XRD patterns. Profile D is indexed taking account the coexistence of hexagonal IBN-9 and cubic MCM-48 (indices shown in parentheses).

dx.doi.org/10.1021/cm2023983 | *Chem.Mater.* 2011, 23, 5250−5255

CTAB is one of the most popularly used surfactants in materials chemistry for its easy commercial availability,[24−27] and the first template employed for the synthesis of ordered mesoporous materials.[1] It is well-known that under most synthesis conditions, CTAB gives rise to cylindrical MCM-41 structure and only in extreme cases, e.g., with ultrahigh surfactant concentration or pH value, bicontinuous MCM-48 and lamellar MCM-50 structures can be obtained.[1,16] The major difference in templating behavior between S2−C14 and CTAB is that S2−C14 can generate three mesostructures (MCM-41, IBN-9 and MCM-48), whereas CTAB only gives MCM-41 structure under most conditions. This should be attributed to the different molecular geometries of the two surfactants. Compared to CTAB, surfactant S2−C14 has two distinct features in molecular structure, a larger headgroup (a_0) and an additional hydrophobic (phenyl) side group. During the surfactant self-assembly, the side groups tend to enter the hydrophobic micelle core, but because of the linkage to the main chains, they would reside at the hydrophilic−hydrophobic "palisade" region of the micelles. Thus, the volume of the micelles (V) is increased without changing l. The coexistence of two opposing effects (a_0 and V) in the same surfactant allows the packing of surfactant S2−C14 to be finely tuned by other experimental conditions, and this explains the rich mesostructures templated by S2−C14. It is also known that with short-chain alcohol e.g. ethanol, iso-propanol, or *n*-butanol as additive, MCM-48 can be synthesized from CTAB in extensive mild conditions.[16] This is because the medium polarity of the short-chain alcohol molecules makes them reside at the hydrophilic−hydrophobic "palisade" region of CTAB micelles, increasing the micelle volume (V), just like the function of the phenyl group in S2−C14. On the basis of the above-mentioned knowledge from previous studies including (i) IBN-9 is an intermediate structure between MCM-41 and MCM-48, and (ii) the addition of short-chain alcohol into CTAB system can tune the structure from MCM-41 to MCM-48, we rationally propose that IBN-9 may also be synthesized from CTAB by using suitable amount of alcohol as additive under optimized conditions.

To verify this hypothesis, we have carried out a series of syntheses by fixing the concentration of TEOS and CTAB while adjusting the ammonia concentration and the amount of *n*-butanol. As summarized in the synthesis space diagram (Figure 1a), the obtained products can be classified into four categories based on the X-ray diffraction (XRD) results (Figure 1b). When no butanol or a small amount of butanol is added, the product is MCM-41 regardless of the ammonia concentration. With a large amount of butanol (butanol/CTAB molar ratio >40), high-quality MCM-48 can be obtained in a wide range of pH (ammonia concentration), whereas highly concentrated ammonia solution combined with excessive butanol gives rise to disordered structures (Figure 1a). The well-known MCM-41 and MCM-48 structures are explicitly determined from XRD, and disordered structures refer to those exhibiting only one board XRD peak. Three representative synthesis conditions for MCM-41, MCM-48, and the disordered structure are marked in the diagram and the corresponding XRD patterns are shown in Figure 1b(A−C). Interestingly, in a small region of the diagram (butanol/CTAB, 55−65; ammonia concentration, 1−2 wt %), the products exhibit a few XRD peaks that, however, are not well-defined and cannot be assigned to a single structure (Figure 1bD). Compared to the XRD pattern of pure MCM-48 (Figure 1bB), the intense peak in Figure 1bD) is apparently broader with a shoulder peak at lower angle (2θ = 1.98°). We examined the samples from this region with SEM and found two distinct morphologies, i.e., cubic particles and long fibers (Figure 2a).

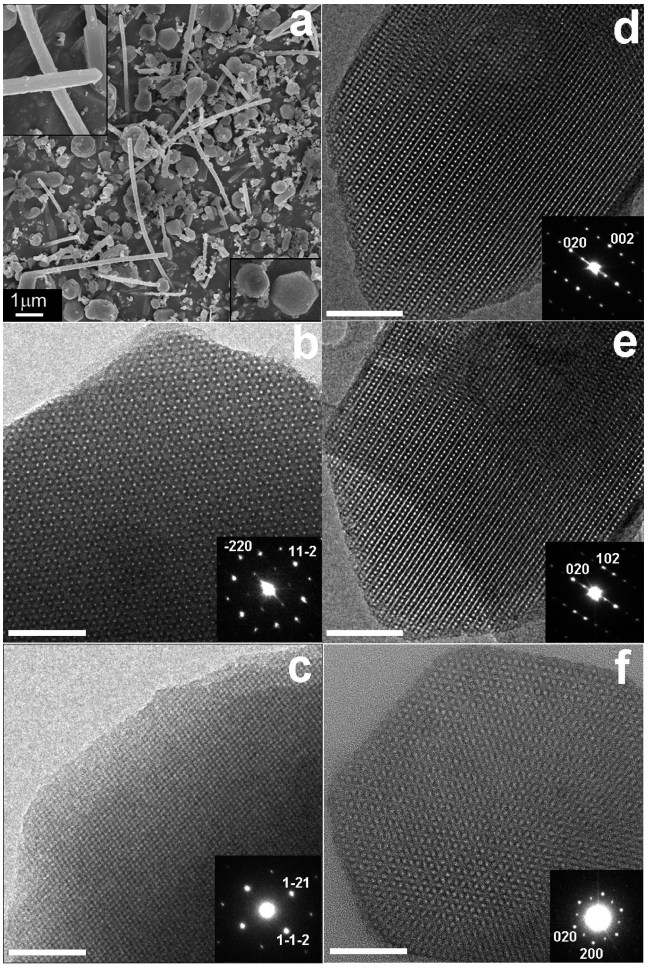

Figure 2. (a) SEM image of the sample prepared from condition D in Figure 1a, showing the coexistence of particles and fibers. The insets are the enlarged representative images of these two morphologies. (b, c) HRTEM images of the particle (MCM-48) taken along the (b) [111] and (c) [531] directions. (d−f) HRTEM images of the fiber (IBN-9) taken along the (d) [100], (e) [201], and (f) [001] directions. The insets of the TEM images are the corresponding SAED patterns. The scale bars in b−f correspond to 50 nm.

Because "morphology" normally reflects the point-group symmetry of the crystal, we speculated that these samples are comprised of cubic MCM-48 and hexagonal IBN-9, corresponding to the particles and fibers, respectively. To confirm this, TEM was applied to examine the particles and fibers separately. The powder was not ground during the TEM specimen preparation to maintain the particles intact, so that the two kinds of morphology could be easily distinguished under TEM. The peripheries of the particles are thin enough for TEM imaging, where highly ordered mesoporous structure characteristic of MCM-48 can be observed. Two typical TEM images shown in Figure 2b, c are taken along the [111] and [531] directions respectively, from which the unit-cell parameter of the MCM-48 is determined to be a = 93.6 Å. On the other hand, the fibers are confirmed to have IBN-9 structure by TEM. Figure 2d shows the TEM image of a single

dx.doi.org/10.1021/cm2023983 | *Chem.Mater.* 2011, 23, 5250−5255

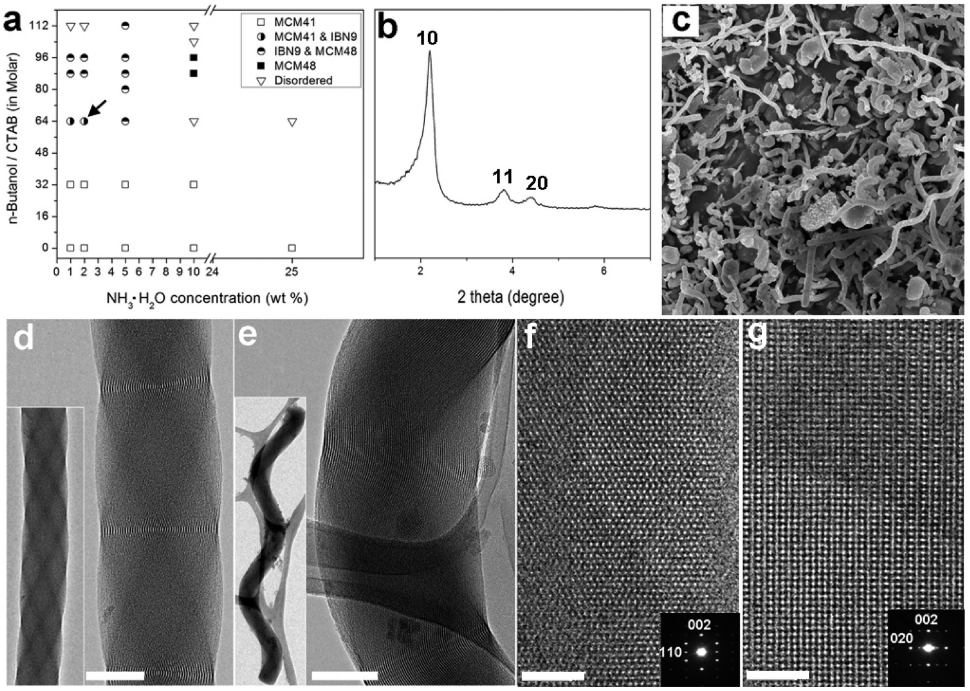

Figure 3. (a) Diagram of mesostructures synthesized from surfactant CTAB with varied amounts of butanol and different ammonia concentrations, where each sample was synthesized using 0.25 mL of TEOS, 30 mg of CTAB in 24 mL of aqueous ammonia solution at 45 °C. The product synthesized from the condition marked by the arrow was characterized by (b) indexed XRD, (c) SEM, and (d–g) TEM. SEM image c shows twisted fibers, spiral fibers and a small quantity of straight fibers. (d, e) HRTEM images of the (d) twisted fiber and (e) spiral fiber. The insets are low-magnification images, showing the fiber morphologies. (f, g) HRTEM images and SAED patterns (insets) of a single straight fiber taken along the (f) $[1\bar{1}0]$ and (g) [100] directions. The scale bars in d–g correspond to 50 nm.

fiber taken along the [100] direction. Tilting the specimen along the *b* axis by ~24° results in the [201] incidence and the obtained TEM image is shown in Figure 2e. Many fibers have been individually examined with TEM and the results show that they all have the same structure. Ultrathin microtome was also applied to cut the particles into thin slices, which provided opportunities to observe the fibers along their long axis direction. In this way, the characteristic [001] fringes of IBN-9 structure can be frequently observed in the TEM specimen (Figure 2f). These results indicate that besides MCM-48, this sample also contains IBN-9 with unit-cell parameters of a = 88.0 Å; c = 84.1 Å. On the basis of the unit cells determined from TEM, the most intense reflection of MCM-48 and the most intense reflection of IBN-9 have very close d values of $d_{\text{MCM-48(211)}}$ = 38.2 Å and $d_{\text{IBN-9(020)}}$ = 38.1 Å. As a result, the major XRD peaks of the two structures overlap and this explains the ill-resolved XRD pattern of their mixture (Figure 1bD). Accordingly, the shoulder peak at 2θ = 1.98° can be assigned to the 110 reflection of IBN-9 structure and the broad peak at 2θ = 2.69° is associated with the overlapping 220 reflection of MCM-48 and 120 reflection of IBN-9 (Figure 1bD). It is hard to accurately determine the proportion of IBN-9 in the mixture that varies with the synthesis conditions. At a rough estimate based on the particle morphologies observed by SEM, the highest proportion of IBN-9 (in weight/volume) that can be achieved by optimizing the synthesis conditions is about 40%.

The synthesis conditions of IBN-9 can be further extended to higher pH region by using less CTAB. Figure 3a shows another diagram where the synthesis conditions are identical to those for Figure 1a except that the amount of CTAB is decreased from 50 mg to 30 mg. Under such conditions, IBN-9 structure appears in a wider range of ammonia concentration (up to 5%). It is reasonable to get IBN-9 structure at higher pH with less CTAB used because as aforementioned increasing the alkalinity of the synthesis media has an opposing effect on the surface curvature of mesostructure against using lower surfactant concentration. However, pure IBN-9 is still unobtainable, and instead it always appears together with its neighboring structures. When higher ammonia concentration and/or larger amount of *n*-butanol are used, the products comprise both IBN-9 and MCM-48, similar to the cases discussed earlier; when lower concentrated ammonia solution and smaller amount of butanol are used, the mixture of IBN-9 and MCM-41 is obtained (Figure 3a). Figure 3c shows a typical SEM image of the latter case, in which three kinds of morphologies i.e. twisted fibers, spiral fibers and straight fibers, can be observed. Further investigation by TEM confirms that the twisted and spiral fibers possess the helical 2-D hexagonal MCM-41 structure that is characterized by the periodical and intermittent lattice fringes along the fiber (Figure 3d, e), as already demonstrated thoroughly in previous studies.[28−32] On the other hand, the straight fibers are determined to be IBN-9, for instance, the [100] and $[1\bar{1}0]$ TEM images of a single straight fiber are shown in Figure 3f, g, respectively, which were taken sequentially by tilting the specimen along the fiber long axis by 30°. According to SEM and TEM observation, MCM-41 is the major product, whereas the proportion of IBN-9 in the mixture is estimated to be <10%. This is consistent with the XRD pattern that does not show visible peaks associated with the tricontinuous mesostructure (Figure 3b). These results clearly indicate that with the help of *n*-butanol the tricontinuous IBN-9 structure can be fabricated from CTAB under extensive

dx.doi.org/10.1021/cm2023983 | *Chem.Mater.* 2011, 23, 5250–5255

conditions and provide additional proof that IBN-9 is an intermediate between MCM-41 and MCM-48 (Figure 3a).

Besides *n*-butanol, we attempted to use other short-chain alcohols including *n*-propanol, iso-propanol, and ethanol as additives with alcohol/CTAB molar ratio of 50−200 and ammonia concentration of 1−5 wt %. The products were exclusively MCM-41 as determined by XRD and TEM. Notably, IBN-9 structure can only be synthesized under static condition. Stirring conditions result in either MCM-41 or MCM-48, depending on the surfactant concentration. The same applies to the special surfactant S2−C14 system.[19] This suggests that compared to MCM-41 and MCM-48, IBN-9 structure is less thermodynamically stable and its formation may be associated with kinetic factors such as the diffusion rate and concentration gradient of the silicate precursor that affect the rate of crystal growth. Recent studies reported the transition between bicontinuous D structure and G structure and electron crystallography results indicated that the former has slightly higher surface mean curvature and smoother silica wall.[35,36] The present CTAB/*n*-butanol system allows the simultaneous formation of bicontinuous G structure (MCM-48) and tricontinuous H structure (IBN-9), thus providing a suitable platform for thoroughly investigating the transition between bicontinuous and tricontinuous mesostructures.

CONCLUSIONS

In this study, we successfully synthesize the tricontinuous mesoporous silica IBN-9 using commercially available surfactant CTAB with the help of *n*-butanol that allows the surface curvature of the organic/inorganic interface to be finely tuned to generate intermediate structure. Although the synthesis of pure IBN-9 is not achieved, it has been demonstrated that this very complicated mesoporous structure can be fabricated from the most popular and simplest surfactant system. Actually, the use of short-chain alcohols with CTAB or other surfactants to synthesize MCM-48 was reported many years ago.[16,33,34] Looking back on those syntheses, we suspect that most likely IBN-9 structure had been obtained in some cases as a minor product, but was ignored. This is possibly because at that time, people intended to get bicontinuous MCM-48 without knowing the existence of tricontinuous structure. When different components are mixed, people often see only what they expect to see while ignoring things that may be more interesting. Thanks to our specially designed surfactant S2−C14 that enables the synthesis of pure IBN-9, it makes it easy to identify it to be a new structure and to resolve it, and in turn allows us to find that the same structure can be generally fabricated with simpler and commercially available surfactants.

AUTHOR INFORMATION

Corresponding Author

*E-mail: yu.han@kaust.edu.sa. Tel: +966-544700032.

ACKNOWLEDGMENTS

This work was supported by the Global Collaborative Research AEA program from King Abdullah University of Science and technology.

REFERENCES

(1) Beck, J. S.; Vartuli, J. C.; Roth, W. J.; Leonowicz, M. E.; Kresge, C. T.; Schmitt, K. D.; Chu, C. T. W.; Olson, D. H.; Sheppard, E. W. *J. Am. Chem. Soc.* **1992**, *114*, 10834−10843.
(2) Zhao, D. Y.; Feng, J. L.; Huo, Q. S.; Melosh, N.; Fredrickson, G. H.; Chmelka., B. F.; Stucky., G. D. *Science* **1998**, *279*, 548−552.
(3) Zhao, D. Y.; Huo, Q. S.; Feng, J. L.; Chmelka, B. F.; Stucky, G. D. *J. Am. Chem. Soc.* **1998**, *120*, 6024−6036.
(4) Fan, G.; Yu, C. Z.; Gao, F.; Lei, J.; Tian, B. Z.; Wang, L. M.; Luo, Q.; Tu, B.; Zhou, W. Z.; Zhao, D. Y. *Angew. Chem., Int. Ed.* **2003**, *42*, 3146−3150.
(5) Carlsson, A.; Kaneda, M.; Sakamoto, Y.; Terasaki, O.; Ryoo, R.; Joo., S. H. *J. Electron Microsc.* **1999**, *48*, 795−798.
(6) Gao, C.; Sakamoto, Y.; Sakamoto, K.; Terasaki, O.; Che, S. *Angew. Chem., Int. Ed.* **2006**, *45*, 4295−4298.
(7) Finnefrock, A. C.; Ulrich, R.; Du Chesne, A.; Honeker, C. C.; Schumacher, K.; Unger, K. K.; Gruner, S. M.; Wiesner, U. *Angew. Chem., Int. Ed.* **2001**, *40*, 1208−1211.
(8) Che, S.; Garcia-Bennett, A. E.; Yokoi, T.; Sakamoto, K.; Kunieda, H.; Terasaki, O.; Tatsumi, T. *Nat. Mater.* **2003**, *2*, 801−805.
(9) Han, Y.; Lee, S. S.; Ying, J. Y. *Chem. Mater.* **2007**, *19*, 2292−2298.
(10) Ryoo, R.; Joo, S. H.; Jun, S. *J. Phys. Chem. B* **1999**, *103*, 7743−7746.
(11) Inagaki, S.; Guan., S.; Ohsuna, T.; Terasaki, T. *Nature* **2002**, *416*, 304−307.
(12) Trikalitis, P. N.; Rangan, K. K.; Bakas, T.; Kanatzidis, M. G. *J. Am. Chem. Soc.* **2002**, *124*, 12255−12260.
(13) Tian, B. Z.; Liu, X. Y.; Tu, B.; Yu, C. Z.; Fan, J.; Wang, L. M.; Xie, S. H.; Stucky, G. D.; Zhao, D. Y. *Nat. Mater.* **2003**, *2*, 159−163.
(14) Han, Y.; Lee, S. S.; Ying, J. Y. *Chem. Mater.* **2006**, *18*, 643−649.
(15) Feng, X.; Fryxell, G. E.; Wang, L.-Q.; Kim, A. Y.; Liu, J. *Science* **1997**, *276*, 923−926.
(16) Huo, Q. S.; Margolese, D. I.; Stucky, G. D. *Chem. Mater.* **1996**, *8*, 1147−1160.
(17) Israelachvili, J. N.; Mitchell, D. J.; Ninham, B. W. *J. Chem. Soc., Faraday Trans. II* **1976**, *72*, 1525−1568.
(18) Hyde, S. T. *Pure Appl. Chem.* **1992**, *64*, 1617−1622.
(19) Han, Y.; Zhang, D. L.; Chng, L. L.; Sun, J. L.; Zhao, L.; Zou, X. D.; Ying, J. Y. *Nat. Chem.* **2009**, *1*, 121−127.
(20) Zhao, Y. F.; Zhang, D. L.; Zhao, L.; Wang, G. C.; Zhu, Y. H.; Cairns, A.; Sun., J. L.; Zou, X. D.; Han, Y. *Chem. Mater.* **2011**, *23*, 3775−3786.
(21) Zhang, D. L.; Sun, J. L.; Han, Y.; Zou, X. D. *Microporous Mesoporous Mater.* **2011**, *146*, 88−96.
(22) Hyde, S. T.; Schröder, G. E. *Curr. Opin. Colloid Interface Sci.* **2003**, *8*, 5−14.
(23) Wan, Y.; Zhao, D. Y. *Chem. Rev.* **2007**, *107*, 2821−2860.
(24) Wang, H.; Levin, C. S.; Halas, N. J. *J. Am. Chem. Soc.* **2005**, *127*, 14992−14993.
(25) Gou, X. L.; Cheng, F. Y.; Shi, Y. H.; Zhang, L.; Peng, S. J.; Chen, J.; Shen, P. W. *J. Am. Chem. Soc.* **2006**, *128*, 7222−7229.
(26) Wang, L. Y.; Chen, X.; Zhan, J.; Chai, Y. C.; Yang, C. J.; Xu, L. M.; Zhuang, W. C.; Jing, B. *J. Phys. Chem. B* **2005**, *109*, 3189−3194.
(27) Jiang, X. M.; Brinker, C. J. *J. Am. Chem. Soc.* **2006**, *128*, 4512−4513.
(28) Che, S. A.; Liu, Z.; Ohsuna, T.; Sakamoto, K.; Terasaki, O.; Tatsumi, T. *Nature* **2004**, *429*, 281−284.
(29) Ohsuna, T.; Liu, Z.; Che, S. A.; Terasaki, O. *Small* **2005**, *1*, 233−237.
(30) Han, Y.; Zhao, L.; Ying, J. Y. *Adv. Mater.* **2007**, *19*, 2454−2459.
(31) Yang, S.; Zhao, L. Z.; Yu, C. Z.; Zhou, X. F.; Tang, J. W.; Yuan, P.; Chen, D. Y.; Zhao, D. Y. *J. Am. Chem. Soc.* **2006**, *128*, 10460−10466.
(32) Yuan, P.; Zhao, L. Z.; Liu, N.; Wei, G. F.; Zhang, Y.; Wang, Y. H.; Yu, C. Z. *Chem.—Eur. J.* **2009**, *15*, 11319−11325.
(33) Liu, S.; Cool, P.; Collart, O.; Van Der Voort, P.; Vansant, E. F.; Lebedev, O. I.; Van Tendeloo, G.; Jiang, M. *J. Phys. Chem. B* **2003**, *107*, 10405−10411.
(34) Kim, T.-W.; Kleitz, F.; Paul, B.; Ryoo, R. *J. Am. Chem. Soc.* **2005**, *127*, 7601−7610.
(35) Miyasaka, K.; Terasaki, O. *Angew. Chem., Int. Ed.* **2010**, *49*, 8867−8871.

(36) Han, L.; Miyasaka, K.; Terasaki, O.; Che, S. *J. Am. Chem. Soc.* **2011**, *133*, 11524−11533.